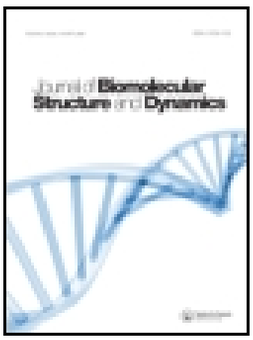

Taylor & Francis
Taylor & Francis Group

Journal of Biomolecular Structure and Dynamics

ISSN: (Print) (Online) Journal homepage: https://www.tandfonline.com/loi/tbsd20

Anti-glycemic potential of benzophenone thio/semicarbazone derivatives: synthesis, enzyme inhibition and ligand docking studies

Arshia, Sharmeen Fayyaz, Muniza Shaikh, Khalid Mohammed Khan & M. Iqbal Choudhary

To cite this article: Arshia, Sharmeen Fayyaz, Muniza Shaikh, Khalid Mohammed Khan & M. Iqbal Choudhary (2021): Anti-glycemic potential of benzophenone thio/semicarbazone derivatives: synthesis, enzyme inhibition and ligand docking studies, Journal of Biomolecular Structure and Dynamics, DOI: 10.1080/07391102.2021.1897045

To link to this article: https://doi.org/10.1080/07391102.2021.1897045

View supplementary material

Published online: 26 Mar 2021.

Submit your article to this journal

Article views: 31

View related articles

View Crossmark data

Full Terms & Conditions of access and use can be found at
https://www.tandfonline.com/action/journalInformation?journalCode=tbsd20

JOURNAL OF BIOMOLECULAR STRUCTURE AND DYNAMICS
https://doi.org/10.1080/07391102.2021.1897045

Taylor & Francis
Taylor & Francis Group

Check for updates

Anti-glycemic potential of benzophenone thio/semicarbazone derivatives: synthesis, enzyme inhibition and ligand docking studies

Arshia[a#], Sharmeen Fayyaz[b#], Muniza Shaikh[b], Khalid Mohammed Khan[a,c] and M. Iqbal Choudhary[a,b,d]

[a]H. E. J. Research Institute of Chemistry, International Center for Chemical and Biological Sciences, University of Karachi, Karachi, Pakistan; [b]Dr. Panjwani Center for Molecular Medicine and Drug Research, International Center for Chemical and Biological Sciences, University of Karachi, Karachi, Pakistan; [c]Department of Clinical Pharmacy, Institute for Research and Medical Consultations (IRMC), Imam Abdulrahman Bin Faisal University, Dammam, Saudi Arabia; [d]Department of Chemistry, Faculty of Science and Technology, Universitas Airlangga, Surabaya, Indonesia

Communicated by Ramaswamy H. Sarma

ABSTRACT

Inhibition of dipeptidyl peptidase-IV (DPP-IV) has been identified as a promising approach for the treatment of type 2 diabetes mellitus (T2DM). Therefore, development of DPP-IV inhibitors with new chemical scaffold is of utmost importance to medicinal chemistry. In the present study, we identified benzophenone thio- and semicarbazone scaffolds as novel DPP-IV inhibitors. For that purpose, benzophenone thio- and semicarbazone were synthesized through a 2-step reaction. These newly synthetic derivatives were characterized by different spectroscopic techniques, including HREI-MS and NMR. whereas stereochemistry of the iminic bond was predicted by NOESY experiments. Thio- and semicarbazones derivatives were evaluated for their DPP-IV inhibitory potential and found to exhibit a good to moderate enzyme inhibitory activity. Most active and non-cytotoxic derivatives were further evaluated for their DPP-IV inhibitory potential in *in cellulo* model. The binding sites as well as affinity of active compounds for DPP- IV enzyme were predicted by *in silico* studies, and compared to a standard drug, sitagliptin. Pharmacophore studies of thio- and semicarbazones derivatives 1–29 suggest that substitution of aryl group, particularly a lipophilic substituents at C-4″ of benzene ring, and a hydroxyl at C-4′ strongly influenced the DPP-IV inhibitory activity. Compound 9 showed the highest inhibitory activity ($IC_{50} = 15.0 \pm 0.6\,\mu M$), whereas compounds 10, 17, 12, 14 and 23 showed a moderate activity with IC_{50} values in the range of 28.9–39.2 μM. This study identifies thio- and semicarbazones as new classes of DPP-IV inhibitors which may translate into safe and effective therapeutics for a better management of type 2 diabetes.

ARTICLE HISTORY
Received 26 November 2020
Accepted 24 February 2021

KEYWORDS
Type 2 diabetes mellitus; dipeptidyl peptidase-IV (DPP-IV); thiosemicarbazone; benzophenone; Caco-2 cell line

1. Introduction

Type 2 diabetes mellitus (T2DM) is a complex chronic metabolic disease that is progressive in nature. This disease has acquired an epidemic proportion worldwide in recent years. According to an estimate of World Health Organization (WHO), approximately 422 million people in the world are suffering from diabetes and this number will rise up to 592 million by 2035 (Song et al., 2017). In view of the increasing burden of diabetes and health risks associated with the disease, this is imperative to develop effective, and safe treatments of type 2 diabetes. During the past decade different drugs for the management of type 2 diabetes have been developed, such as inhibition of α-glucosidase enzyme, of anti-glycation drugs, and incretin hormones targeting drugs.

Incretins are gut hormones secreted in response to meal ingestion and triggers glucose-dependent insulin secretion. However, these hormones are instantly degraded by an endogenous enzyme, dipeptidyl peptidase-IV (DPP-IV) (Kato et al., 2018). DPP-IV is, therefore, an important metabolic enzyme, involved in the regulation of glucose levels in serum. It cleaves incretin hormones to their inactive forms which results in an increased level of serum glucose. DPP-IV inhibitors control the glucose level in blood by increasing insulin secretion. Inhibition of DPP-IV, is therefore, an effective strategy for the control of hyperglycemia in T2DM (Xie et al., 2017). Given the increasing prevalence of type 2 diabetes and the substantial social and financial costs associated with disease management, every effort should be made for the prevention and treatment. Over the past years, several DPP-IV inhibitors, such as vildagliptin, sitagliptin, saxagliptin, etc. have been developed. Current DPP-IV inhibitors belong to different chemical classes, however these inhibitors possess primary amine moiety which is responsible for potent DPP-IV inhibition. Unfortunately, these inhibitors suffer some disadvantages, such as short biological half-life (vildagliptin) or a need of larger doses (sitagliptin). Occurrence of

CONTACT M. Iqbal Choudhary iqbal.choudhary@iccs.edu H. E. J. Research Institute of Chemistry, International Center for Chemical and Biological Sciences, University of Karachi, Karachi 75270, Pakistan
#These authors contribute equally in this work and shared first authorship.

Supplemental data for this article can be accessed online at https://doi.org/10.1080/07391102.2021.1897045

© 2021 Informa UK Limited, trading as Taylor & Francis Group

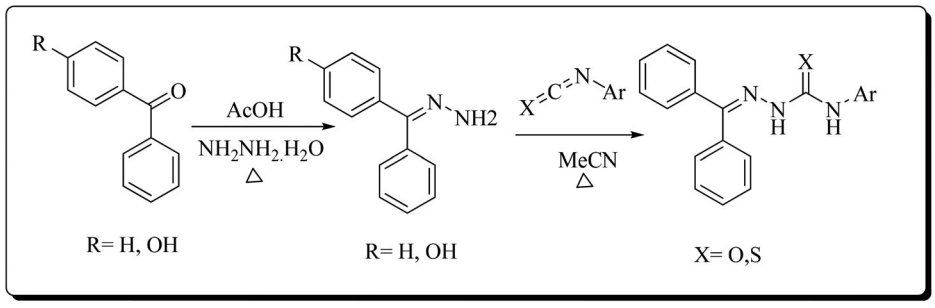

Scheme 1. Synthesis of benzophenone thio- and semicarbazones.

pancreatitis and pancreatic cancer is also observed with administration of DPP-IV inhibitors (Baig et al., 2019; Prabahar et al., 2020). This encouraged investigation of the chemical space for the identification of lead molecules against this clinically important enzyme with lower side effects, and increased inhibitory potential.

The cost effective synthesis of thio- and semicarbazones derivatives and their importance in drug designing have attracted the attention of many researchers. These are known to possess many important biological activities, such as antimicrobial, antimalarial (Kpomah, 2017), antifungal, anticancer (Divar et al., 2017), anti-inflammatory, antioxidant, antitumor (Kalaiarasi et al., 2017), antituberculosis (Kaplancı klı et al., 2016), antiepileptic (Rajak et al., 2017), antiproliferative (Zaltariov et al., 2017), antiglycating, antioxidant, (Arshia et al., 2020) and antileishmanial properties (Silva & Silva, 2017). There are several studies demonstrating the anti-diabetic effect of thiosemcarbazones as aldose reductase and glycogen phosphorylase inhibitors (Alexacou et al., 2010; Kulkarni et al., 2012; Shehzad et al., 2019). Recently, Sever et al. (2020) reported the DPP-IV inhibitory effect of pyrazole incorporated thiosemicarbazone derivatives.

In the present study, we identified benzophenone-based thio- and semicarbazone as DPP-IV inhibitors by high throughput screening. *In situ* cellular assay using Caco-2 cell line further indicates the potential of identified leads in complex physiological environment. Inhibitors identified during this research can serve as leads for further research in this important field.

2. Experimental

2.1. Material and methods

Acetic acid, hydrazine hydrates, benzophenones and different aryl isocyanates/isothiocyantes were purchased from Sigma Aldrich, USA. Acetonitrile was dried by charging it with 3 Å molecular sieves. Recombinant human DPP-IV (EC 3. 4. 14. 5) was purchased from Prof. Dr. Mark D. Gorrell, Sydney, Australia. Sitagliptin phosphate monohydrate (S4002) was purchased from Selleck Chemicals (TX, USA). Gly-pro-*p*NA was obtained from LeapChem Ltd. (Hangzhou, China). Dulbecco's modified eagle medium (DMEM) was purchased from Cassion Labs, USA. All solvents (DMSO and ethanol) were of HPLC grade.

NMR spectra were recorded on Avance Bruker AM 300 and 400 MHz spectrometers. EI-MS were run on a Finnigan MAT-311A (Germany) mass spectrometer. Melting points of the compounds were recorded on Stuart® SMP10 melting point apparatus. IR spectra (KBr discs) were recorded on a FTS 3000 MX, Bio-RAD Merlin (Excalibur Model) spectrophotometer. Thin layer chromatography (TLC) analyses were performed on pre-coated silica gel aluminum plates (Kieselgel 60, 254, E. Merck, Germany). TLC chromatograms were visualized under ultraviolet lamp at 254 and 365 nm.

2.2. Synthesis of thio- and semicarbazone derivatives

Synthesis and characterization of compounds **1**–**8**, **15–23**, **25–27** and **29** are reported previously by Arshia et al. (2016), and same methodology is used for the synthesis of compounds **9–14**, **24** and **28**. Briefly, benzophenone semicarbazones and thiosemicarbazones were synthesized by refluxing benzophenone hydrazones and substituted aryl isocyanates or isothiocyanates in acetonitrile for 24 h (Scheme 1). Completion of reaction was confirmed by TLC analysis. Synthetic mixtures were then left at room temperature for precipitation. The precipitates were filtered and dried under vacuum at 40 °C to afford good yields of the desired compounds. The compounds, were crystallized from ethanol.

2.2.1. Characteristics spectral features of synthesized derivatives

2.2.1.1. (E)-N-(2-Chlorophenyl)-2-((4-hydroxyphenyl)(phenyl)methylene)hydrazinecarbothioamide (9). Yield: 75%; m.p. 177–179 °C; R_f: 0.35 (ethyl acetate/hexanes, 2:8); ^{1}H NMR (400 MHz, DMSO-d_6): δ_H 10.34 (d, 1H, NH)), 10.04 (d, 1H, NH), 9.09 (d, 1H, OH), 7.71 (d, 2H, $J_{2,3/6,5} = 7.6$ Hz, H-2, H-6), 7.66 (m, 2H, H-4, H-5″), 7.56 (t, 2H, $J_{3(2,4)/5(4,6)} = 7.6$ Hz, H-3, H-5), 7.40 (m, 4H, H-2′, H-3′, H-5′, H-6′), 7.21 (d, 1H, $J_{4(3,5)} = 6.8$ Hz, H-4), 7.02 (d, 1H, $J_{6'',5''} = 8.8$ Hz, H-6″), 6.77 (d, 1H, $J_{3'',4''} = 8.8$ Hz, H-3″); FAB-MS *m/z* 382 $[M+H]^+$, 384 $[M+H+2]^+$.

2.2.1.2. (E)-N-(3-Chlorophenyl)-2-((4-hydroxyphenyl)(phenyl)methylene)hydrazine carbothioamide (10). Yield: 72%; m.p. 144–146 °C; R_f: 0.34 (ethyl acetate/hexanes, 2:8); ^{1}H NMR (300 MHz, DMSO-d_6): δ_H 10.42 (d, 1H, NH), 10.06 (d, 1H, NH),

9.04 (d, 1H, NH), 7.73 (d, 2H, $J_{2,3/6,5} = 7.6$ Hz, H-2, H-6), 7.65 (d, 1H, $J_{4(3,5)} = 6.8$ Hz, H-4), 7.57 (m, 2H, H-3, H-5), 7.41 (m, 4H, H-2′, H-3′, H-5′, H-6′), 7.28 (m, 1H, H-2″), 7.20 (d, 1H, $J_{5''(4'',6'')} = 9.0$ Hz, H-5″), 7.02 (d, 1H, $J_{6'',5''} = 9.0$ Hz, H-6″), 6.78 (d, 1H, $J_{4'',5''} = 9.0$ Hz, H-4″); EI-MS: *m/z* (rel. abund.%) 383 $[M^+ + 2]$ (15.5), 381 $[M]^+$ (38.0), 348 (5.4), 304 (6.8), 254 (100.0), 211 (55.3), 196 (100.0), 169 (8.0), 152 (13.7), 127 (87.2), 92 (13.1), 77 (42.5), 51 (9.2); HREI-MS: *m/z* $C_{20}H_{16}ClN_3OS$ $[M]^+$ 381.0703, found 381.0702.

2.2.1.3. (E)-N-(4″-Chlorophenyl)-2-((4-hydroxyphenyl)(phenyl)methylene)hydrazinecarbothioamide (11).

Yield: 79%; m.p. 198–200 °C; R_f: 0.33 (ethyl acetate/hexanes, 2:8); ^{1}H NMR (400 MHz, DMSO-d_6): δ_H 10.39 (d, 1H, NH), 10.05 (d, 1H, OH), 8.97 (d, 1H, NH), 7.72 (d, 1H, $J_{4(3,5)} = 6.8$ Hz, H-4), 7.65 (m, 4H, H-2, H-6, H-6′, H-2′), 7.48 (m, 3H, H-6″, H-3′, H-5′), 7.38 (t, 2H, $J_{3(2,4)/5(4,6)} = 8.8$ Hz, H-3, H-5), 7.20 (d, 1H, $J_{5'',6''} = 8.0$ Hz, H-5″), 7.02(d, 1H, $J_{3'',5''} = 8.4$ Hz, H-3″), 6.77 (d, 1H, $J_{2'',3''} = 8.4$ Hz, H-2″); EI-MS: *m/z* (rel. abund.%), 383 $[M^+ + 2]$ (3.3), 381 $[M]^+$ (5.5), 254 (35.0), 211 (11.3), 196 (100.0), 181 (20.8),169 (22.9), 127 (90.8), 106 (64.0), 77 (32.2), 65.0 (27.9); HREI-MS: *m/z* Calcd $C_{20}H_{16}ClN_3OS$ $[M]^+$ 381.0703, found 381.0702.

2.2.1.4. (E)-N-(2″-Fluorophenyl)-2-((4′-hydroxyphenyl)(phenyl)methylene)hydrazinecarbothioamide (12).

Yield: 77%; m.p. 120–122 °C; R_f: 0.34 (ethyl acetate/hexanes, 2:8); ^{1}H NMR (400 MHz, DMSO-d_6): δ_H 10.23 (d, 1H, NH), 10.03 (d, 1H, NH), 9.02 (d, 1H, OH), 7.73 (d, 1H, $J_{4(3,5)} = 6.8$ Hz, H-4), 7.66 (m, 2H, H-2, H-6), 7.55 (d, 2H, $J_{2',3'/6',5'} = 8.8$ Hz, H-2′, H-6′), 7.41 (m, 4H, H-3, H-5, H-3′, H-5′), 7.26 (d, 1H, $J_{5''(4'',6'')} = 8.8$ Hz, H-5″), 7.02 (d, 1H, $J_{6'',5''} = 8.8$ Hz, H-6″), 6.76 (d, 1H, $J_{3'',4''} = 8.8$ Hz, H-3″); EI-MS: *m/z* (rel. abund.%), 365 $[M]^+$ (89.2), 332 (15.9), 288 (12.0), 254 (93.0), 211 (8.9),196 (100.0), 181 (22.5), 111 (59.5), 77 (29.0); HREI-MS: *m/z* Calcd $C_{20}H_{16}FN_3OS$ $[M]^+$ 365.0998, found 365.0997.

2.2.1.5. (E)-N-(3″-Fluorophenyl)-2-((4-hydroxyphenyl)(phenyl)methylene)hydrazinecarbothioamide (13).

Yield: 75%; m.p. 144–146 °C; R_f: 0.34 (ethyl acetate/hexanes, 2:8); ^{1}H NMR (400 MHz, DMSO-d_6): δ_H 10.40 (d, 1H, NH), 10.04 (d, 1H, NH), 8.76 (d, OH), 7.72 (m, 3H, H-3, H-4, H-5), 7.55 (d, 2H, $J_{2,3} = J_{6,5} = 6.6$ Hz, H-2, H-6), 7.42 (d, 2H, $J_{2',3'/6',5'} = 6.3$ Hz, H-2′, H-6′), 7.36 (m, 2H, H-2″, H-5″), 7.20 (d, 1H, $J_{4'',5''} = 6.3$ Hz, H-4″), 7.06 (m, 2H, H-3′, H-5′), 6.78 (d, 1H, $J_{6'',5''} = 6.6$ Hz, H-6″); EI-MS: *m/z* (rel. abund.%), 365 $[M]^+$ (42.0), 288 (9.6), 254 (65.1), 211 (65.2), 196 (100.0), 152 (53.7), 120 (32.5), 111 (94.3), 77 (96.8); HREI-MS: *m/z* Calcd $C_{20}H_{16}FN_3OS$ $[M]^+$ 365.0998, found 365.0997.

2.2.1.6. (E)-N-(2″-Bromophenyl)-2-((4-hydroxyphenyl)(phenyl)methylene)hydrazinecarbothioamide (14).

Yield: 77%; m.p. 158–160 °C; R_f: 0.35 (ethyl acetate/hexanes, 2:8); ^{1}H NMR (400 MHz, DMSO-d_6): δ_H 10.32 (d, 1H NH), 10.03 (d, 1H, OH), 9.08 (d, 1H, NH), 7.71 (d, 2H, $J_{2,3/6,5} = 6.8$ Hz, H-2, H-6), 7.66 (m, 2H, H-3, H-5), 7.54 (d, 1H, $J_{4\ (3,5)} = 8.4$ Hz, H-4), 7.43 (m, 4H, H-2′, H-3′, H-5′, H-6′), 7.25 (m, 2H, H-4, H-5″), 7.02 (d, 1H, $J_{6'',5''} = 8.4$ Hz, H-6″), 6.77 (d, 1H, $J_{3'',4''} = 8.4$ Hz, H-3″), 2.06 (s, 3H, 2″-CH_3″); FAB-MS *m/z* 426 $[M + H]^+$, 428 $[M + H + 2]^+$.

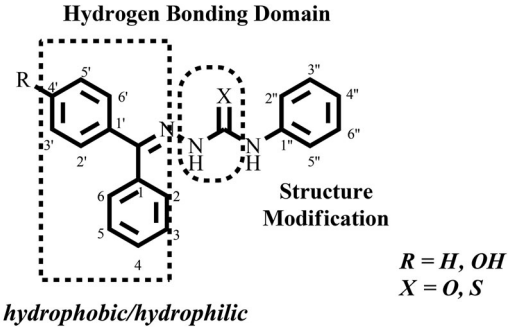

Figure 1. Structural features of newly synthesized thio- and semi-carbazones derivatives.

2.2.1.7. N-(4-Chloro-2-(trifluoromethyl)phenyl)-2-(diphenylmethylene)hydrazinecarboxamide (24).

Yield: 69%; m.p. 185–187 °C; R_f: 0.38 (ethyl acetate/hexanes, 2:8); ^{1}H NMR (300 MHz, DMSO-d_6): δ_H 9.85 (s, 1H, NH), 9.37 (s, 1H, NH), 9.15 (s, 1H, OH), 8.15 (s, 1H, H-3″), 7.76 (d, 2H, $J_{2,3} = J_{6,5} = 9.0$ Hz, H-2, H-6), 7.56 (m, 5H, H-3, H-5, H-4, H-2′, H-6′), 7.29 (m, 1H, H-5), 7.15 (d, 2H, $J_{3',2'} = J_{5',6'} = 8.7$ Hz, H-3′, H-5′), 6.95 (d, 1H $J_{6'',5''} = 8.4$ Hz, H-6″), 6.77 (d, 1H $J_{5'',6''} = 8.7$ Hz, H-5″); ^{13}C NMR: (100 MHz, DMSO-d_6): δ_C 158.45, 153.00, 152.20, 149.71, 137.69, 135.18, 135.16, 133.20, 132.82, 130.13, 129.38, 128,74, 128.35, 127.55, 127.09, 125.98, 122.28, 116.12, 115.23, 115.20, 110.91; EI-MS: *m/z* (rel. abund.%): $[M^+ + 2]$ 419 (3.3), $[M]^+$ 417 (13.0), 221 (29.3), 211 (56.7), 195 (100.0), 175 (63.3), 43 (74.4); HREI-MS: *m/z* Calcd for $C_{20}H_{16}ClN_3O_2$ $[M]^+$ 433.0805, found 433.0808; IR (KBr, cm^{-1}): 3344 (O–H), 3278 (N–H), 1691 (C = O), 1589 (C = N), 1589 (C = C), 1311 (C–N), 839 (C–F).

2.2.1.8. (E)-N-[4″-Chloro-2″-(trifluoromethyl)phenyl]-2-[(4′-hydroxyphenyl)(phenyl)methylene] hydrazinecarboxamide (28).

Yield: 69%; White solid; m.p. 172–174 °C; R_f: 0.37 (ethyl-acetate/hexanes, 2:8); ^{1}H NMR (300 MHz, DMSO-d_6): δ_H 9.85 (s, 1H, NH), 9.37 (s, 1H, NH), 9.15 (s, 1H, OH), 8.15 (s, 1H, H-3″), 7.76 (d, 2H, $J_{2,3} = J_{6,5} = 9.0$ Hz, H-2, H-6), 7.56 (m, 5H, H-3, H-5, H-4, H-2′, H-6′), 7.29 (m, 1H, H-5), 7.15 (d, 2H, $J_{3',2'} = J_{5',6'} = 8.7$ Hz, H-3′, H-5′), 6.95 (d, 1H $J_{6'',5''} = 8.4$ Hz, H-6″), 6.77 (d, 1H $J_{5'',6''} = 8.7$ Hz, H-5″); ^{13}C NMR: (100 MHz, DMSO-d_6): δ_C 158.4 (C = O), 152.2 (C = N), 149.7 (C-4′), 137.6 (C-4″), 135.1 (C-2″), 133.2 (C-1″), 130.1 (C-3″), 129.3 (C-1), 128.7 (C-5″), 128.5 (C-6″), 128.3 (C-2, C-6), 127.5 (C-3, C-5), 127.0 (C-4), 125.9 (C-2′, C-6′), 122.2 (C-1′), 116.1 (2′-CF_3), 115.2 (C-3′, C-5′); EI-MS: *m/z* (rel. abund.%): $[M^+ + 2]$ 435 (3.2), 433 $[M]^+$ (9.2), 416 (1.4), 221 (29.3), 211 (56.7), 195 (100.0), 175 (63.3), 43 (74.4); HREI-MS: *m/z* Calcd for $C_{20}H_{16}ClN_3O_2$ $[M]^+$ 433.0805, found 433.0808; IR (KBr, cm^{-1}): 3344 (O–H), 3278 (N–H), 1691(C = O), 1589 (C = N), 1589 (C = C), 1311 (C–N), 839 (C–F). ^{1}H NMR spectra of newly synthetic derivatives are given in Supplementary Materials.

2.3. DPP-IV Inhibitory assay

DPP-IV inhibitory activity of compounds **1**–**29** was evaluated using gly-pro-pNA as chromogenic substrate. Release of *p*-nitroanilide, a light yellow colored compound, due to cleavage of substrate by the DPP-IV enzyme was monitored.

Table 1. DPP-IV inhibitory potential of thio/semicarbazone derivatives **1**–**29**.

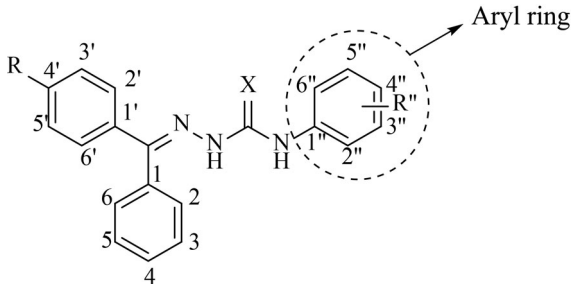

Compounds	Structure			IC_{50} ± SEM[a] (μM)
	X	R	R″	
1	S	H	Phenyl	NA[b]
2	S	H	3″-Chloro	NA
3	S	H	2″,5″-Dichloro	NA
4	S	H	2″,3″- Dichloro	NA
5	S	H	3″,4″-Dichloro	NA
6	S	H	4″-Bromo	NA
7	S	H	3″-Bromo	NA
8	S	OH	H	69.9 ± 1.01
9	S	OH	2″-Chloro	15.0 ± 0.6
10	S	OH	3″-Chloro	38.27 ± 1.84
11	S	OH	4″-Chloro	79.0 ± 1.3
12	S	OH	2″-Fluoro	28.9 ± 0.32
13	S	OH	3″-Fluoro	73.0 ± 0.27
14	S	OH	2″-Bromo	34.0 ± 2.06
15	S	OH	3″-Bromo	49.6 ± 0.07
16	S	OH	4″-Bromo	161.7 ± 6.47
17	S	OH	2″,5″-Dichloro	39.2 ± 1.55
18	S	OH	2″,3″-Dichloro	NA
19	S	OH	2″,4″-Dichloro	NA
20	O	H	H	43.5 ± 0.44
21	O	H	3″-Chloro	NA
22	O	H	3″-Trifluoromethyl	NA
23	O	H	4″-Trifluoromethyl	37.46 ± 0.97
24	O	H	2″-Trifluoromethyl-4″-chloro	NA
25	O	H	2″-Chloro-5″-trifluoromethyl	66.04 ± 0.77
26	O	OH	3″-Chloro	NA
27	O	OH	4″-Trifluoromethyl	87.5 ± 0.7
28	O	OH	2″-Trifluoromethyl-4″-chloro	136.4 ± 2.89
29	O	OH	2″-Chloro-5″-trifluoromethyl	59.37 ± 0.17
Sitagliptin (standard)				0.033 ± 0.4

[a]SEM, standard error of mean of three experiments.
[b]NA, not active at 0.2 mM.

Compounds were dissolved in DMSO and diluted in assay buffer (Tris-HCl, pH 8.0). Sitagliptin was used as the reference drug (Hsu et al., 2015; Tanwar et al., 2014). Reaction mixture contain 35 μL of test samples along with 15 μL of enzyme (0.025 units/mL). After 20 min incubation at 37 °C, 50 μL of 0.2 mM substrate was added and changes in absorbance was recorded continuously for 60 min at 400 nm using Spectramax M5 (Molecular Devices, CA, USA). Experiments were carried out in triplicates (Nongonierma et al., 2013).

2.4. Human colorectal adenocarcinoma cell (Caco-2) culture and maintenance

Caco-2 cell line (ATCC-HTB37) was purchased from American Type Culture Collection (ATCC). DMEM supplemented with 1% non-essential amino acids (Sigma-Aldrich, Germany) and 10% fetal bovine serum was used as a growth medium. Cells were cultured at 37 °C and 5% CO_2 atmosphere. Medium was changed after two days, until cells reached confluence (Brandt et al., 2005).

2.5. In situ Caco-2 cell DPP-IV inhibition assay

DPP-IV inhibition assay using Caco-2 cellular model was performed with slight modifications, as described by Sadir et al. (2004). Caco-2 cells were used as a source of DPP-IV enzyme. Caco-2 cells were seeded at a density of 1×10^5 cells per well in a 96-well flat-bottom plate in 200 μL of Dulbecco's modified eagle medium. At confluency, cell culture medium was removed and cells were washed with sterile phosphate buffer, followed by the addition of 50 μL of test sample prepared in HEPES buffer (20 mM, pH 7.4). Cells were incubated further at 37 °C for 4 h, prior to the addition of the substrate Gly-Pro-pNA (0.2 mM). Enzymatic activity was determined by monitoring the release of *p*NA in the supernatant with spectrophotometry at 400 nm using Spectramax M5 (Molecular Devices, CA, USA) (Sadir et al., 2004).

2.6. Molecular docking studies

For docking analysis, the X-ray crystal structure of human DPP-IV (PDB ID 1 × 70), complexed with sitagliptin, was retrieved from PDB. The crystal structure of the protein is a homodimer of subunits A and B. The subunit A was retained for protein preparation by *Protein Preparation Wizard* in Maestro Schrodinger (2019). The co-crystallized water molecules were deleted and the missing hydrogens were added. Assignment of partial charges was carried out *via* OPLS3e force field. Restrained minimization was carried out in order to optimize the heavy atoms and hydrogens in the refine tab of preparation wizard.

Compounds **9** and **14** were sketched in ChemDraw and then converted to their respective 3D structures through the L*ig Prep* module of Maestro (Schrodinger, 2019a). The compounds were further corrected for their protonation and ionization states in the same module by using OPLS3e force field.

Prior to docking, the receptor grid was generated by selecting the co-crystallized sitagliptin molecule as centroid to define the volume of the docking grid. The docking was performed in Glide extra precision (XP) mode based on OPLS3e force field (Friesner et al., 2004, 2006; Halgren et al., 2004; SchrÖdinger, 2019b), where the protein was kept rigid and ligands were kept flexible. The docking protocol was further validated by docking the sitagliptin in the binding site of DPP-IV. The docking reproduced the pose of co-crystallized sitagliptin (Figure S1(a)). The molecular interactions were also reproduced after docking of sitagliptin (Figure S1(b)).

2.7. Statistical analysis

All the experiments were carried out in triplicate and processed using SoftMax Pro 4.8 software (Molecular Devices, CA, USA). Results are expressed as mean ± standard error of

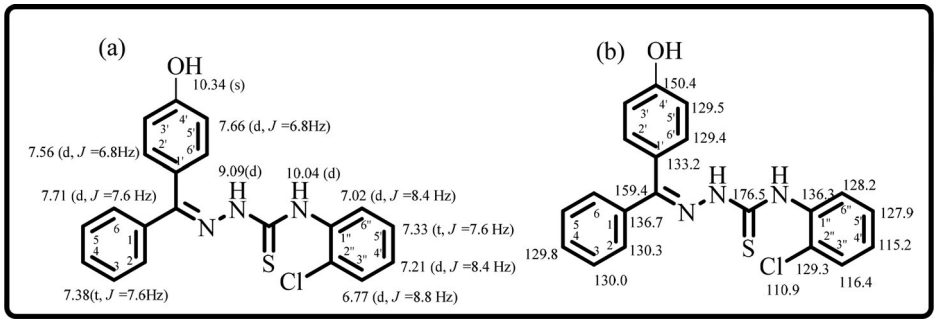

Figure 2. ^{1}H (a), ^{13}C NMR (b) chemical shifts of compound **9**.

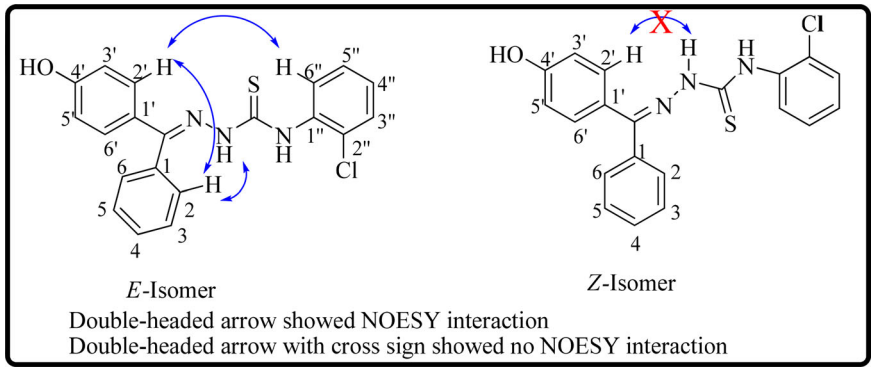

Figure 3. Distinctive NOESY interaction.

mean. IC_{50} values were calculated using EZ-FIT enzyme kinetics software (Perrella Scientific Inc., NH, USA).

3. Results and discussion

3.1. Spectroscopic studies of compound (E)-N-(2-chlorophenyl)-2-((4-hydroxyphenyl)(phenyl)methylene)hydrazinecarbothioamide (9)

Detailed characterization of structures of synthetic benzophenone thio- and semicarbazone derivatives was accomplished. The structure elucidation of compound **9** is presented here as a representative example, since it is most active compound of synthetic series. Important structural features and binding sites of of all other derivatives are shown in Figure 1.

NMR spectroscopy was performed to elucidate the structure 9. ^{1}H and ^{13}C NMR spectra were recorded in deuterated DMSO on Bruker-Avance AM 400 and 500 MHz instruments, respectively. In ^{1}H NMR, two NH protons and one phenolic OH protons resonate at δ_H 10.34, 10.04 and 9.09, respectively. However, protons of non-hydroxybenzene ring of benzophenone resonated as a doublet at δ_H 7.71 ($J_{2,3} = J_{6,5} = 7.6$ Hz, H-2, H-6) and the other ring protons resonated as a triplet at δ_H 7.38 (t, 3H, $J_{3(4,5)/4(3,5)/5(4,6)} = 7.6$ Hz. H-3, H-4, H-5). 4′-Hydroxy benzophenone ring also resonated as a doublet at δ_H 7.66 ($J_{3',2'}/_{5',6'} = 6.8$ Hz, H-3′, H-5′) and at δ_H 7.56 ($J_{2',3'}/_{6',5'} = 6.8$ Hz, H-2′, H-6′). In addition, H-5″ resonated as triplet at δ_H 7.33 ($J_{5''(6'',4'')} = 7.6$ Hz, H-5″) and H-4″, H-6″, H-3″ resonated as doublets at δ_H 7.21 ($J_{4'',3''} = 8.4$ Hz, H-4″), 7.02 ($J_{6'',5''} = 8.4$ Hz, H-6″), 6.77 ($J_{3'',5''} = 8.8$ Hz, H-3″), respectively (Figure 2(a)).

In broad-band ^{13}C NMR spectrum of compound **9**, sixteen (16) signals are appeared. Out of these seven (7) are due to quaternary carbons. Nevertheless, DEPT-135° and -90° experiments indicated the presence of nine methines and the absence of a methylene group. The most down-field signal was of thioamidic carbon at δ_C 176.5. The iminic carbon resonated at δ_C 159.4. Aromatic carbon with OH substituent (C-4′) resonated at δ_C 150.4. Aromatic carbon with chloro substituents (C-2″) resonated at δ_C 129.3. Remaining aromatic carbons resonated with their respected frequency in the aromatic region (Figure 2(b)).

Mass of compound **9** was calculated by FAB-MS techniques which showed $[M + H]^+$ at *m/z* 382, and $[M+H+2]^+$ 384.

Fourier transform IR (FT-IR) spectrum of compound **9** displayed vibrational frequencies at 3349 cm^{-1} which showed the presence of hydroxyl functionality in the compound. Absorbance at 3269 cm^{-1} showed NH functionality. Aromatic (C = C) functionalities vibrated at 1539 cm^{-1}. However, C–N and C–Cl bonds vibrated at 1367 and 821 cm^{-1}, respectively.

NOESY (nuclear Overhauser enhancement spectroscopy) has been performed on most active compound **9** for the verification of the stereochemical configuration of Schiff base (iminic) double bond. Many interactions were observed in the NOESY spectrum. Strong interaction was observed between iminic NH and H-2 of benzophenone ring which can only be seen in case of *E*-isomer. In the same manner absence of NOESY interaction between iminic NH and H-2′ further validate the *E*-stereochemistry of resulting isomer. Other interactions, such as interactions of H-2/H-2′ and H-2′/H-6″ were also observed (Figure 3).

3.2. Enzyme inhibitory studies

In the current study, we evaluated 29 semicarbazones and thiosemicarbazones (Table 1) for their dipeptidyl peptidase-IV (DPP-IV) inhibitory potential. Results showed that thiosemicarbazones having hydroxyl group at C-4′ of benzophenone ring were more active as compared to their un-substituted analogues **1–7**. This suggests the role of hydroxyl group in the DPP-IV inhibitory activity of these compounds. Strong electron donating effect of –OH may involve in the activation of benzophenone ring system for π–π interactions with the aromatic amino acids in the active site of enzyme. Arshia et al. have also reported that hydroxyl group at C-4′ of thiosemicarbazones is vital for enzyme inhibitory activity against jack bean (*Canavalia ensiformis* (L.)) urease. It was also noted that thiosemicarbazone showed stronger DPP-IV inhibitory activity than semicarbazones.

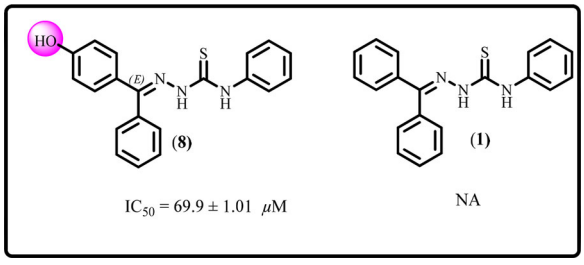

Figure 4a. Structure–activity relationship of thiosemicarbazone analogs with non-substituted substituted aryl part.

Thiosemicarbazone **8** with a hydroxyl group at C-4 and un-substituted phenyl ring showed only a weak inhibitory activity ($IC_{50} = 69.9 \pm 1.01$ μM) as compared to standard drug ($IC_{50} = 0.033 \pm 0.4$ μM). Whereas compound **1**, which lacks the hydroxyl group, was found inactive (Figure 4a).

Substitution of halogens at different positions of phenyl ring resulted in altered enzyme inhibitory activity of thiosemicarbazone derivatives. Compound **9** with a chloro group at C-2″ and hydroxyl group at C-4′ showed an IC_{50} value of 15.0 ± 0.6 μM and was found to be the most active member of the series. However, compounds **10** and **11** having chloro

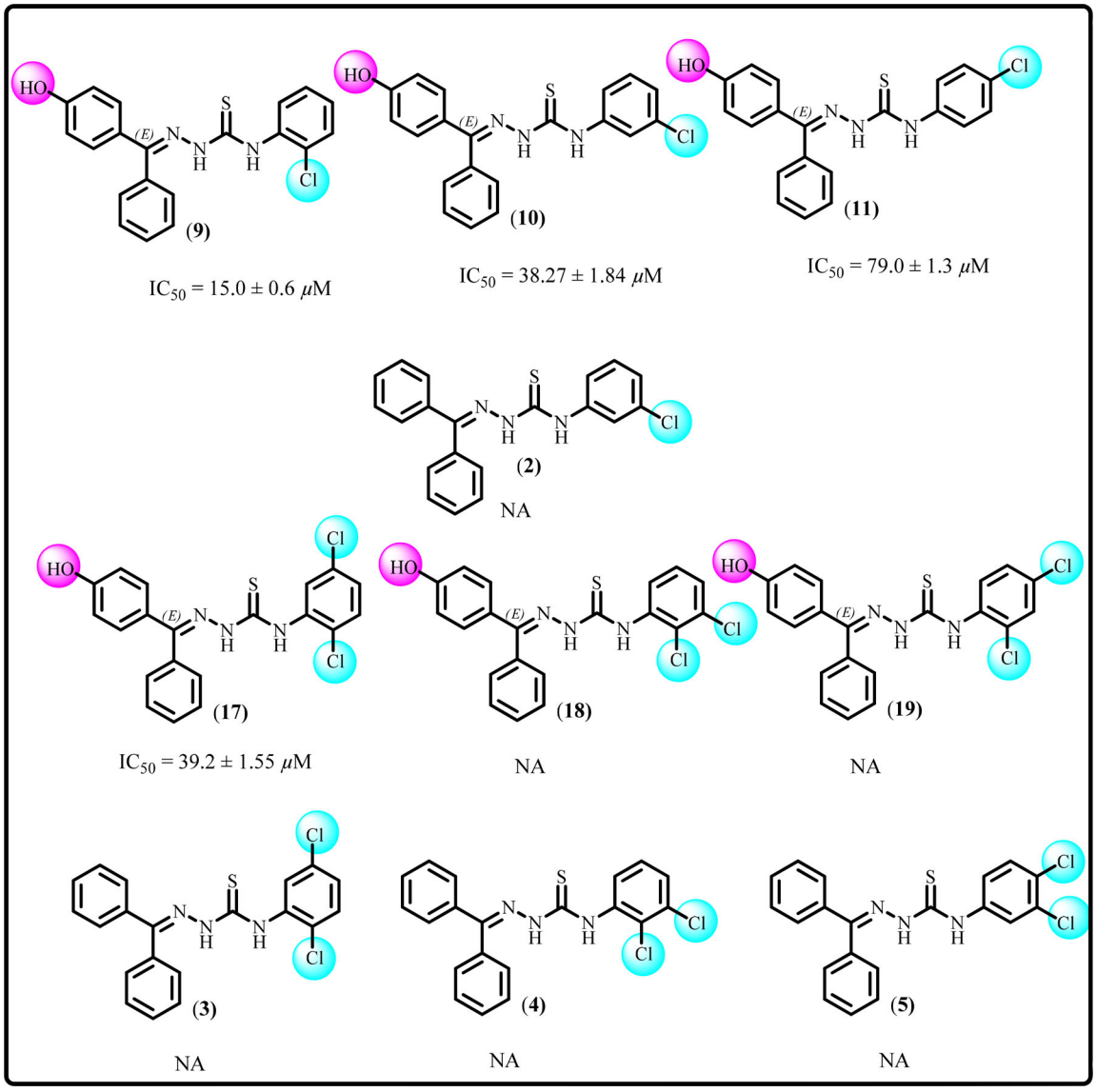

Figure 4b. Structure–activity relationship of thiosemicarbazone analogs with chloro substituted aryl part.

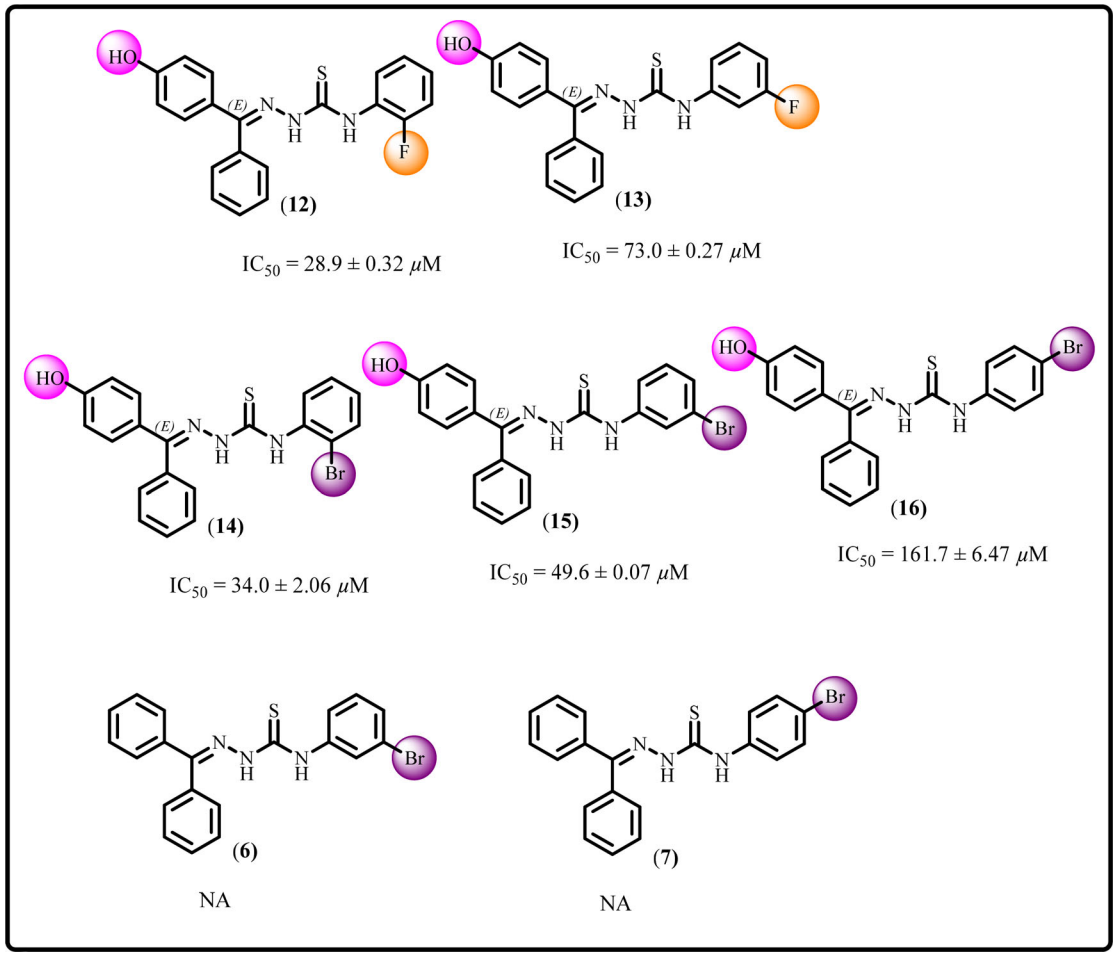

Figure 4c. Structure–activity relationship of thiosemicarbazone analogs with bromo and fluoro substituted aryl part.

group at C-3″ and C-4″, respectively, showed a decreased DPP-IV inhibitory ($IC_{50} = 38.27 \pm 1.84$ and 79.0 ± 1.3 μM, respectively) activity, as compared to the compound **9**. Thiosemicarbazone (**2**) which has chloro group at 3″-position and having no hydroxyl group at 4′-position was found to be completely inactive. Compound **17** having chloro substituents at 2″- and 5″-positions and having hydroxyl group at 4′-position showed only a weak DPP-IV inhibitory activity ($IC_{50} = 39.2 \pm 1.55$ μM). Whereas, compounds **18** and **19** which only differ with chloro group positions were found to be completely inactive. Increased steric bulk in di-chlorinated derivatives **17**, **18** and **19** might be responsible for the weak or inactivity of these compounds against DPP-IV enzyme (Figure 4b).

Thiosemicarbazone (**12**) having fluoro group at C-2″ and a hydroxyl at C-4′ ($IC_{50} = 28.9 \pm 0.32$ μM) showed a moderate enzyme inhibitory activity. However, shifting of fluoro group to C-3″ in compound **13** ($IC_{50} = 73.0 \pm 0.27$ μM) resulted in a decreased activity. Similar trend was observed in compounds **14** and **15** where a decrease in DPP-IV inhibitory activity was observed when bromo group is shifted from C-2″ ($IC_{50} = 34.0 \pm 2.06$ μM) to C-3″ ($IC_{50} = 49.6 \pm 0.07$ μM), respectively. Further decrease in enzyme inhibitory activity was observed in compound **16** where bromo group is present at C-4″ ($IC_{50} = 161.7 \pm 6.47$ μM). However, compounds **6** and **7** showed no inhibition of DPP-IV enzyme, irrespective of the position of bromo group, which might be attributed to the absence of hydroxyl group at C-4′ (Figure 4c). These results suggested that halogen substituent at *ortho* position are more active than those with *meta* substituted derivatives, and they are more active than their analogues at *para* position. Halogens at *ortho* position might increase the electrophilicity of the thioamide group for possible interaction with the hydroxyl group of serine in the active site of DPP-IV enzyme, which may have resulted in an increased enzyme inhibitory activity.

Moderate to weak enzyme inhibition was observed in semicarbazone derivatives. Interestingly, inhibitory potential of semicarbazone derivatives depend on the position of trifluoromethyl group rather than the hydroxyl group at C-4′. Compound **20**, a semicarbazone with an un-substituted phenyl ring, showed a moderate enzyme inhibitory activity ($IC_{50} = 43.5 \pm 0.44$ μM). Compounds **21** and **26** with a –Cl at C-3″ were found to be inactive, irrespective of C-4′ substitution. Compounds **22**, bearing a trifuoromethyl groups at C-3″, was found to be inactive. However, when trifluoromethyl was present at C-4 ″ in compounds **23** and **27** a moderate enzyme inhibition was observed (IC_{50} values 37.46 ± 0.97 and 87.5 ± 0.7 μM, respectively). The only structural difference was the presence of –OH group at C-4′ in compound **27** which

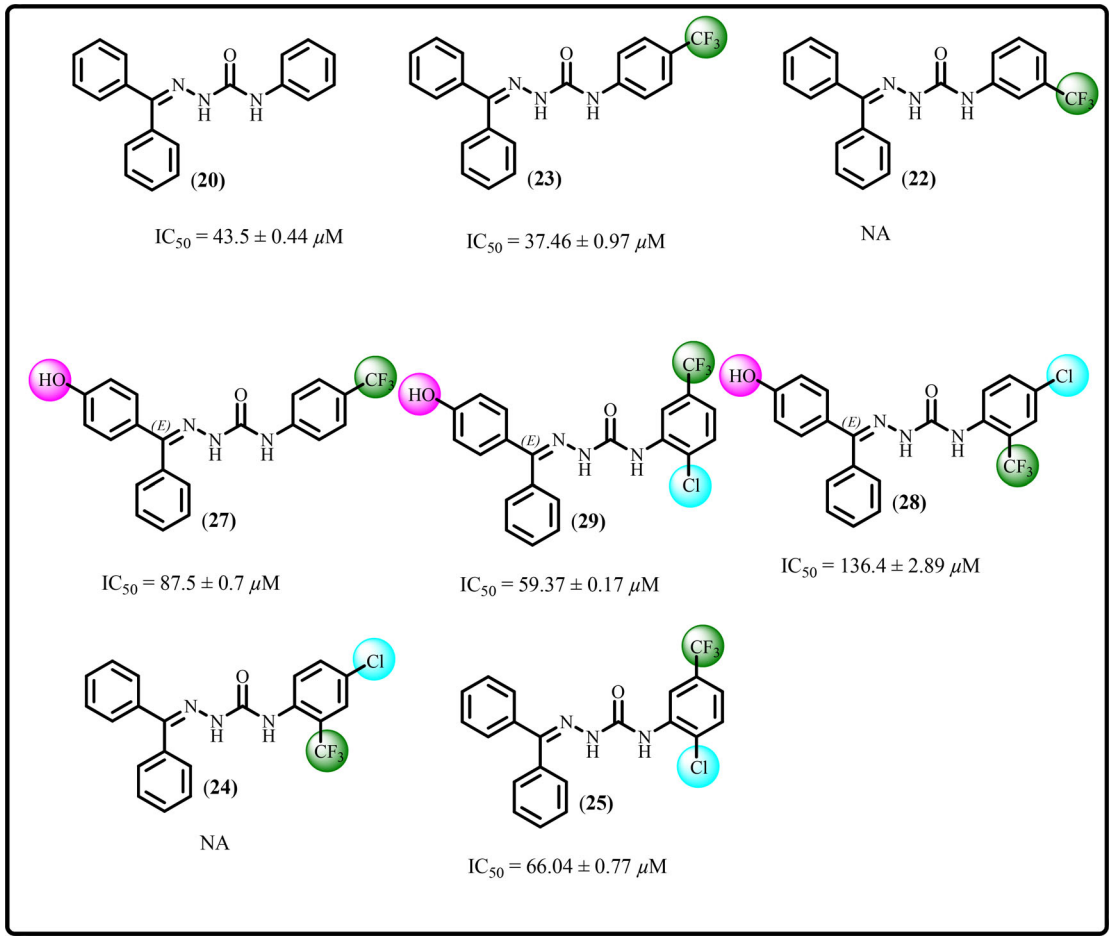

Figure 4d. Structure–activity relationship of semicarbazone analogs with chloro and trifluoromethyl substituted aryl part.

resulted in a decreased inhibitory potential of this compound. Comparable inhibition was observed in compounds **25** and **29** (IC_{50} = 66.04 ± 0.77, and 59.37 ± 0.17 μM, respectively). Strong electron donating effect of chloro group when present at *ortho* position of benzene, might be responsible of the observed inhibitory activities of these analogues. Compound **28** showed only a weak inhibition of DPP-IV enzyme (IC_{50} = 136.4 ± 2.89 μM). This compound is substituted with a trifluoromethyl at *ortho* and a chloro group is present at *para* position. However, the effect of these substitutions was only visible only when a hydroxyl group was at C-4′ of benzophenone ring. Though compound **24** bearing same substitution at aryl part but lacks a hydroxyl group at C-4′ of benzophenone part was found to be inactive (Figure 4d).

Hence, preliminary SAR studies revealed that trifluoromethyl, halogen substitutions, C-4′ hydroxyl and CONH/CSNH are particularly important for the inhibition of enzyme DPP-IV. Combined effect of these groups may influence the binding ability of these molecules with amino acid residues present in the active site or hydrophobic pocket of enzyme DPP-IV. Synthesis of more derivatives with structural variations and validation of identified inhibitors using *in vivo* models and molecular mechanistic studies will be required to demonstrate the efficacy of these leads for the inhibition of DPP-IV enzyme.

3.3. Molecular docking studies

The compounds that were found to be active against DPP-IV in *in vitro* biochemical assay were subjected to docking studies to decipher their molecular interactions. DPP-IV is a homodimer consisting of subunits A and B. These subunits are further divided into α/β-hydrolase and β-propeller domains. The enzyme is a type-II transmembrane protein with the membrane-spanning region from 7 to 28 amino acid residues. The α/β-hydrolase domain starts with amino acids 39–51 and 506–766 and is closest to the membrane. While the β-propeller domain consists of residues 55–497.

As sitagliptin is used as reference drug in the *in vitro* assay, docking pose of identified inhibitors were also compared to the reference drug. The crystal structure used for docking analysis is 1x70, co-crystallized with the drug sitagliptin (Figure 5(a) and (b)). It is a recombinant sequence deprived of membrane-spanning region. The *N*-terminal region of 1x70 starts with Ser39, which is the soluble form of the protein found in plasma.

The co-crystallized sitagliptin in the DPP-IV binding site showed hydrogen bondings with the carboxyl and hydroxyl groups of Glu205 and Tyr662, respectively. The trifluorophenyl and triazole moieties of sitagliptin made π–π interactions with the phenol ring of Tyr666 and benzene moiety of Phe357 Figures 6, and S2.

Compounds **9** and **14** were found to be most active against DPP-IV with IC_{50} values 15.0 ± 0.6 and 34.06 ± 2.06 μM, respectively, and hence chosen for docking studies.

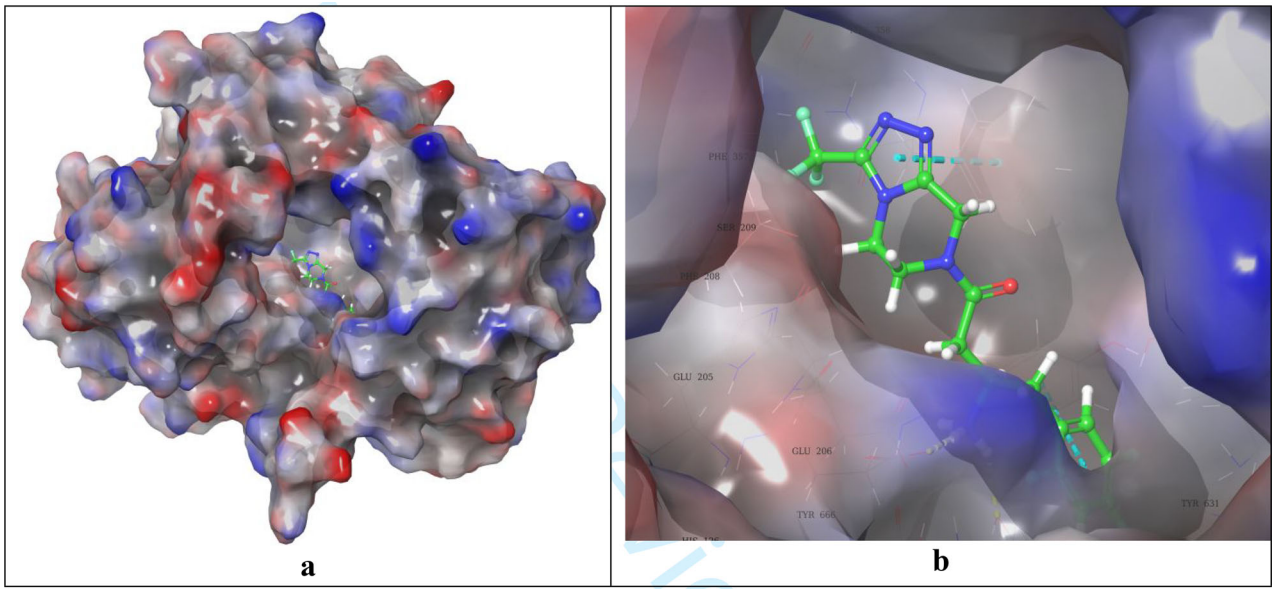

Figure 5. (a) 3D Molecular surface representation of DPP-IV (PDB ID: 1X70) prepared by *protein* preapartion *wizard* tool illustrating the overall structure of enzyme. (b) The co-crystalized sitagliptin depicting the binding pose in the active site.

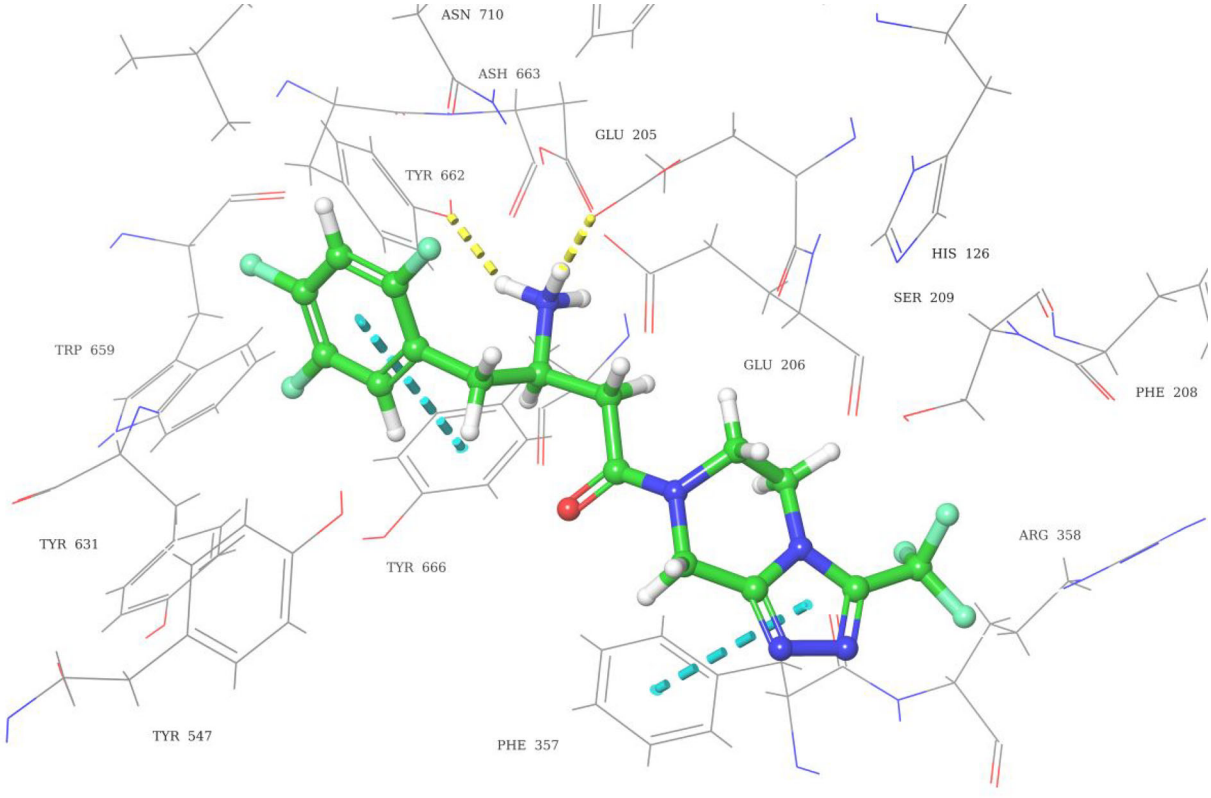

Figure 6. Modelled posed of drug sitagliptin in the binding site of DPP-IV (PDB ID: 1X70).

Docking of compound **9** in the binding site of DPP-IV showed π–π interactions with Tyr666 and Phe357 through its benzene moieties. While the hydroxyl benzyl moiety form hydrogen bonding interaction with His126 figures 7, and S3.

Compound **14** showed a flip in the orientation of the docked pose, as compared to compound **9**. The bromobenzene moiety formed π–π interactions with the indole moiety of Trp629. A halogen bond was also observed with guanidinum group of Arg125. The hydroxyl benzyl moiety interacted through hydrogen bonds with Glu205 Figures 8. and S4. The molecular interactions of these compounds along with sitagliptin in the binding site of DPP-IV are summarized in Table S1.

3.4. Cytotoxicity studies

Mouse fibroblast 3T3 cells were used for initial cytotoxic evaluation. Most active compounds **8–15**, **17**, **20**, **23**, **26**, **27**

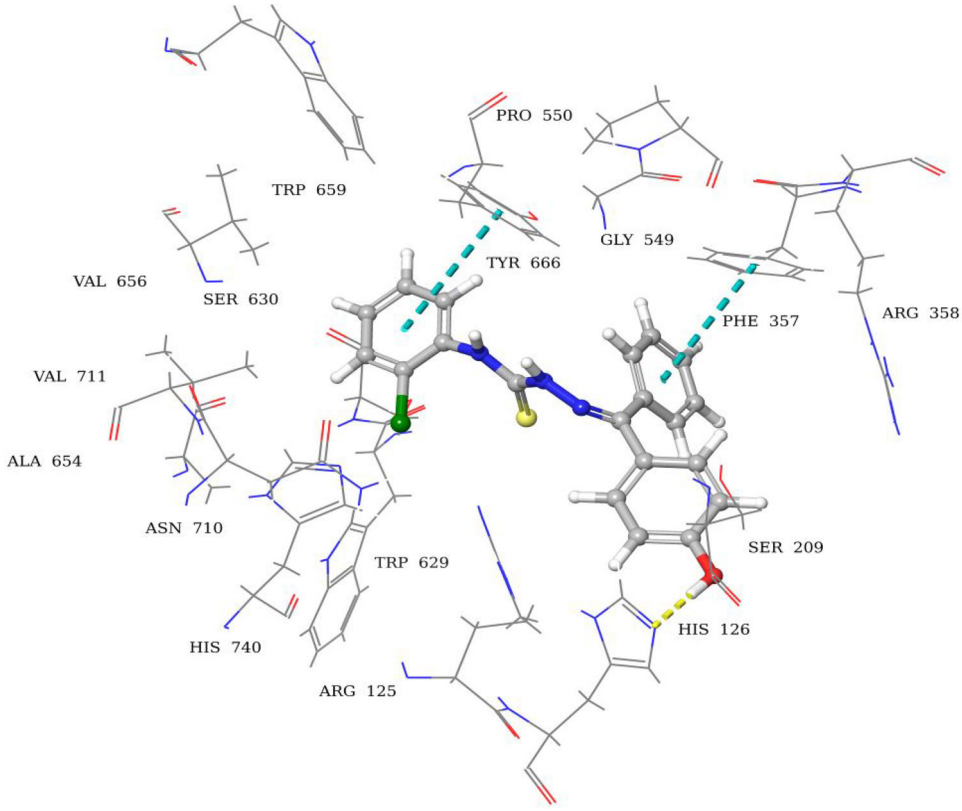

Figure 7. Docked pose of compound **9** in the binding site of enzyme DPP-IV. Hydrogen bonds are represented as yellow dotted lines. π–π interaction is represented as cyan dotted lines.

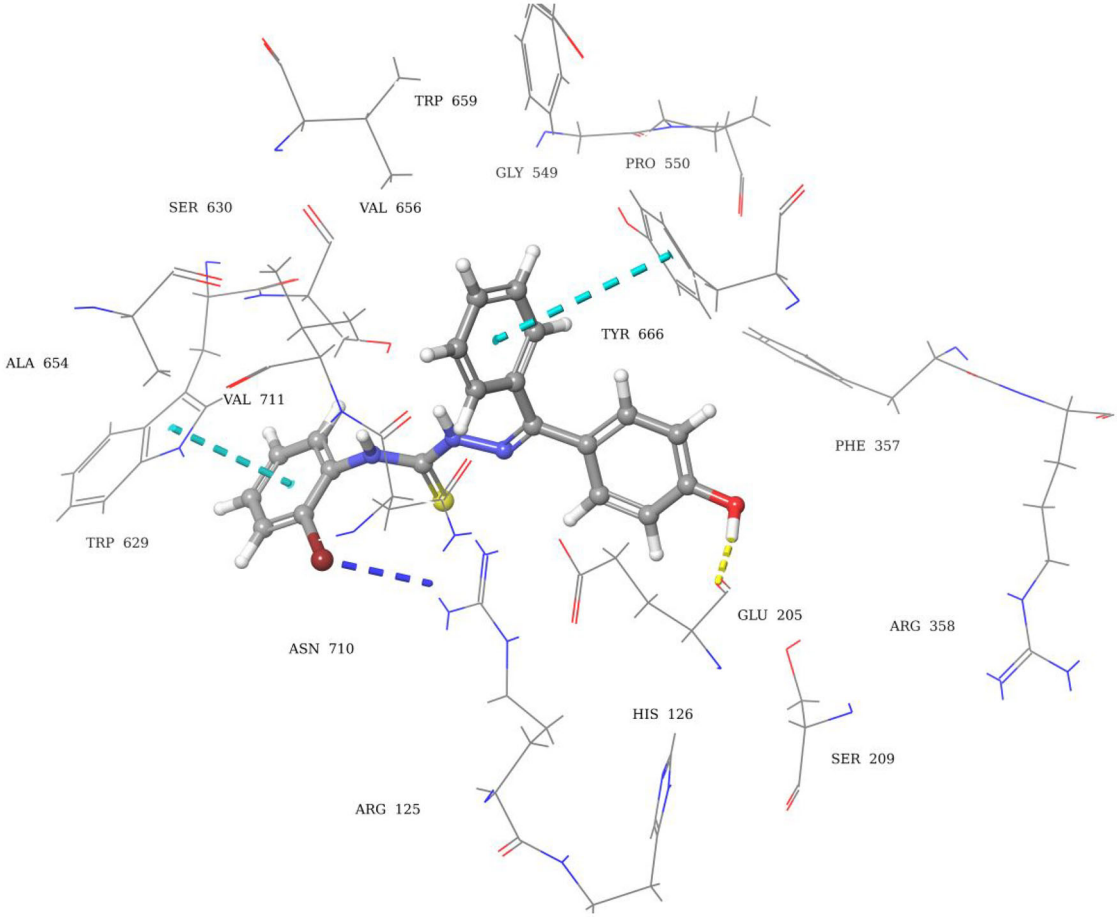

Figure 8. Docked pose of compound **14** in the binding site of enzyme DPP-IV. Hydrogen bonds are represented as yellow dotted lines. π–π interaction is represented as cyan dotted lines.

and **29** were evaluated for their cytotoxicity. Compounds **8**, **14**, **17,** and **27** showed a weak cytotoxicity with IC_{50} values 19.0 ± 0.2, 27.8 ± 1.9, 25.7 ± 0.3, and 24.6 ± 0.3 μM, respectively. Whereas compound **29** was found to be highly cytotoxic (IC_{50} = 8.2 ± 0.5 μM) against this cell line. All other compounds were found non-cytotoxic.

3.5. Inhibition of DPP-IV *in* in situ *Caco-2 cellular assay*

Inhibitors identified through *in vitro* studies sometimes do not correlate in *in vivo* models, because standard enzyme inhibition assays with purified enzymes do not stimulate certain factors that might affect inhibitor's bioactivity. We, therefore, further evaluated the efficacy of our identified inhibitors using Caco-2 cellular assay. It has been reported that Caco-2 cell line expresses many membrane bound enzymes, and hence is a reliable model for toxicity testing, drug absorption and proteolytic activity of enzymes (Caron et al., 2017). Use of DPP-IV specific substrate confirmed the expression of DPP-IV in confluent Caco-2 cells.

Compounds **9**, **10**, **12**, **14**, **17**, **20,** and **23** were evaluated for their DPP-IV inhibitory activity in cellular model. Only compounds **9** and **14** (IC_{50} = 55.6 ± 9.8 and 94.9 ± 0.1 μM, respectively) inhibited DPP-IV enzyme in *in situ* cellular (*in cellulo*) assay. These results are in agreement with our results of *in vitro* DPP-IV inhibition assay which showed that thiosemicarbazones with a hydroxyl at C-4′ and halogen at C-2″ have favorable configuration for predictive interactions with DPP-IV active sites. IC_{50} value of standard drug, sitagliptin, was found to be 7.6 ± 0.72 μM in *in situ* Caco-2 DPP-IV inhibition assay.

Our results for the first time demonstrated the inhibitory potential of benzophenone based thio- and semicarbazone derivatives against DPP-IV enzyme. However, these are preliminary results, and further studies are required to optimize the inhibitory activity and to study the underlying mechanism for the inhibition.

4. Conclusion

In conclusion, we report here benzophenone-based thiosemicarbazone and semicarbazone derived DPP-IV inhibitors. Insights into the structure–activity relationship reveals that halogen substituents, *ortho* to thioamide (compounds **9**, **12,** and **14**) are contributing significantly in the inhibitory activity of DPP-IV. As for the semicarbazone derivatives, we observed that trifluoromethyl is mainly responsible for the enzyme inhibitory activity. Varied enzyme inhibitory activities, showed by thio- and semicarbazone derivatives can be correlated with different aryl substitutions, as well as hydroxyl group at C-4′ of benzophenone part. Furthermore evaluation of the potential inhibitors in *in situ* Caco-2 assay demonstrated their inhibitory potential under intestinal cell conditions. These compounds offer excellent starting point for medicinal chemists to explore new chemical scaffolds and optimize existing chemical entities with improved therapeutic profile. Further optimization of these compounds for better efficacy lead to the development of novel therapeutic agents for type 2 diabetes with minimal side effects.

Disclosure statement

No potential conflict of interest was reported by the authors.

Funding

Authors are grateful to the Higher Education Commission (HEC), Pakistan, for providing financial support under the Indigenous Ph.D. Fellowship for 5000 Scholars Phase-II program and Pakistan Academy of Sciences for financial support to Project No. 5-9/PAS/440.

References

Alexacou, K.-M., Tenchiu Deleanu, A.-C., Chrysina, E. D., Charavgi, M.-D., Kostas, I. D., Zographos, S. E., Oikonomakos, N. G., & Leonidas, D. D. (2010). The binding of β-d-glucopyranosyl-thiosemicarbazone derivatives to glycogen phosphorylase: A new class of inhibitors. *Bioorganic & Medicinal Chemistry*, *18*(22), 7911–7922. https://doi.org/10.1016/j.bmc.2010.09.039

Arshia, A., Khan, A., Khan, K. M., Saad, S. M., Siddiqui, N. I., Javaid, S., Perveen, S., & Choudhary, M. I. (2016). Synthesis and urease inhibitory activities of benzophenone semicarbazones/thiosemicarbazones. *Medicinal Chemistry Research*, *25*(11), 2666–2679. https://doi.org/10.1007/s00044-016-1673-0

Arshia, Abbasi, S., Rasheed, S., Khan, J. A., Saad, S. M., Khan, K. M., & Choudhary, M. I. (2020). *In vitro* antiglycation and antioxidant properties of benzophenone thiosemicarbazones. *Pakistan Journal of Pharmaceutical Sciences*, *33*(3), 1147–1153.

Baig, M. M. F. A., Naveed, M., Abbas, M., Chunxia, W., Ullah, S., Hasnat, M., Shad, A., Sohail, M., Khan, G. J., & Ansari, M. T. (2019). DNA scaffold nanoparticles coated with HPMC/EC for oral delivery. *International Journal of Pharmaceutics*, *562*, 321–332. https://doi.org/10.1016/j.ijpharm.2019.03.054

Brandt, I., Joossens, J., Chen, X., Maes, M. B., Scharpé, S., De Meester, I., & Lambeir, A. M. (2005). Inhibition of dipeptidyl-peptidase IV catalyzed peptide truncation by vildagliptin ((2S)-{[(3-hydroxyadamantan-1-yl)amino]acetyl}-pyrrolidine-2-carbonitrile). *Biochemical Pharmacology*, *70*(1), 134–143. https://doi.org/10.1016/j.bcp.2005.04.009

Caron, J., Domenger, D., Dhulster, P., Ravallec, R., & Cudennec, B. (2017). Using Caco-2 cells as novel identification tool for food-derived DPP-IV inhibitors. *Food Research International (Ottawa, Ont.)*, *92*, 113–118. https://doi.org/10.1016/j.foodres.2017.01.002

Divar, M., Khalafi-Nezhad, A., Zomorodian, K., Sabet, R., Faghih, Z., Jamali, M., Pournaghz, H., & Khabnadideh, S. (2017). Synthesis of some novel semicarbazone and thiosemicarbazone derivatives of isatin as possible biologically active agents. *Journal of Pharmaceutical Research International*, *17*(6), 1–13. https://doi.org/10.9734/JPRI/2017/35243

Friesner, R. A., Banks, J. L., Murphy, R. B., Halgren, T. A., Klicic, J. J., Mainz, D. T., Repasky, M. P., Knoll, E. H., Shelley, M., Perry, J. K., Shaw, D. E., Francis, P., & Shenkin, P. S. (2004). Glide: A new approach for rapid, accurate docking and scoring. 1. Method and assessment of docking accuracy. *Journal of Medicinal Chemistry*, *47*(7), 1739–1749. https://doi.org/10.1021/jm0306430

Friesner, R. A., Murphy, R. B., Repasky, M. P., Frye, L. L., Greenwood, J. R., Halgren, T. A., Sanschagrin, P. C., & Mainz, D. T. (2006). Extra precision glide: Docking and scoring incorporating a model of hydrophobic enclosure for protein–ligand complexes. *Journal of Medicinal Chemistry*, *49*(21), 6177–6196. https://doi.org/10.1021/jm051256o

Halgren, T. A., Murphy, R. B., Friesner, R. A., Beard, H. S., Frye, L. L., Pollard, W. T., & Banks, J. L. (2004). Glide: A new approach for rapid, accurate docking and scoring. 2. Enrichment factors in database screening. *Journal of Medicinal Chemistry*, *47*(7), 1750–1759. https://doi.org/10.1021/jm030644s

Hsu, C. Y., Sulake, R. S., Huang, P.-K., Shih, H.-Y., Sie, H.-W., Lai, Y.-K., Chen, C., & Weng, C. F. (2015). Synthetic (+)-antroquinonol exhibits dual actions against insulin resistance by triggering AMP kinase and inhibiting dipeptidyl peptidase IV activities. *British Journal of Pharmacology*, *172*(1), 38–49. https://doi.org/10.1111/bph.12828

Kalaiarasi, G., Jain, R., Puschman, H., Chandrika, S. P., Preethi, K., & Prabhakaran, R. (2017). New binuclear Ni(II) metallates containing ONS chelators: Synthesis, characterisation, DNA binding, DNA cleavage, protein binding, antioxidant activity, antimicrobial and *in vitro* cytotoxicity. *New Journal of Chemistry*, *41*(7), 2543–2560. https://doi.org/10.1039/C6NJ03516G

Kaplancıklı, Z. A., Altıntop, M. D., Sever, B., Cantürk, Z., & Özdemir, A. (2016). Synthesis and *in vitro* evaluation of new thiosemicarbazone derivatives as potential antimicrobial agents. *Journal of Chemistry*, *2016*, 1–7. https://doi.org/10.1155/2016/1692540

Kato, E., Kawakami, K., & Kawabata, J. (2018). Macrocarpal C isolated from *Eucalyptus globulus* inhibits dipeptidyl peptidase 4 in an aggregated form. *Journal of Enzyme Inhibition and Medicinal Chemistry*, *33*(1), 106–109. https://doi.org/10.1080/14756366.2017.1396458

Kpomah, B. (2017). Spectroscopic characterization, antimicrobial and toxicological properties of derivatised thiosemicarbazone transition metal complexes. *Saudi Journal of Medical and Pharmaceutical Sciences*, *2*(12), 318–325.

Kulkarni, N. V., Revankar, V. K., Kirasur, B. N., & Hugar, M. H. (2012). Transition metal complexes of thiosemicarbazones with quinoxaline hub: An emphasis on antidiabetic property. *Medicinal Chemistry Research*, *21*(5), 663–671. https://doi.org/10.1007/s00044-011-9576-6

Nongonierma, A. B., Mooney, C., Shields, D. C., & Fitzgerald, R. J. (2013). Inhibition of dipeptidyl peptidase IV and xanthine oxidase by amino acids and dipeptides. *Food Chemistry*, *141*(1), 644–653. https://doi.org/10.1016/j.foodchem.2013.02.115

Prabahar, K., Udhumansha, U., & Qushawy, M. (2020). Optimization of thiolated chitosan nanoparticles for the enhancement of *in vivo* hypoglycemic efficacy of sitagliptin in streptozotocin-induced diabetic rats. *Pharmaceutics*, *12*(4), 300. https://doi.org/10.3390/pharmaceutics12040300

Rajak, H., Jain, D. K., Singh, S., Singh, A., K., Patel, V., Veerasamy, R., S., & Pawar, R. (2017). Novel pyrimidine based semicarbazones: Confirmation of four binding site pharmacophoric model hypothesis for antiepileptic activity. *Central Nervous System Agents in Medicinal Chemistry*, *17*(1), 64–71. https://doi.org/10.2174/1871524916666160330122625

Sadir, R., Imberty, A., Baleux, F., & Lortat-Jacob, H. (2004). Heparan sulfate/heparin oligosaccharides protect stromal cell-derived factor-1 (SDF-1)/CXCL12 against proteolysis induced by CD26/dipeptidyl peptidase IV. *The Journal of Biological Chemistry*, *279*(42), 43854–43860. https://doi.org/10.1074/jbc.M405392200

Schrodinger. (2019). 1: Schrödinger Suite 2019-1 Protein Preparation Wizard, Epik,. Schrödinger, LLC. 2019. Impact, Schrödinger, LLC, New York.

Schrodinger. (2019a). Schrödinger Release 2019-1: Glide., Schrödinger, LLC.

Schrodinger. (2019b). Schrödinger Release 2019-1: LigPrep., Schrödinger, LLC.

Sever, B., Soybir, H., Görgülü, Ş., Cantürk, Z., & Altıntop, M. D. (2020). Pyrazole incorporated new thiosemicarbazones: Design, synthesis and investigation of DPP-4 inhibitory effects. *Molecules*, *25*(21), 5003. https://doi.org/10.3390/molecules25215003

Shehzad, M. T., Imran, A., Njateng, G. S. S., Hameed, A., Islam, M., Al-Rashida, M., Uroos, M., Asari, A., Shafiq, Z., & Iqbal, J. (2019). Benzoxazinone-thiosemicarbazones as antidiabetic leads via aldose reductase inhibition: Synthesis, biological screening and molecular docking study. *Bioorganic Chemistry*, *87*, 857–866. https://doi.org/10.1016/j.bioorg.2018.12.006

Silva, B. V., & Silva, B. N. M. (2017). Thio- and semicarbazones: Hope in the search for treatment of leishmaniasis and Chagas disease. *Medicinal Chemistry (Shariqah (United Arab Emirates))*, *13*(2), 110–126. https://doi.org/10.2174/1573406412666160909152614

Song, J. J., Wang, Q., Du, M., Ji, X. M., & Mao, X. Y. (2017). Identification of dipeptidyl peptidase-IV inhibitory peptides from mare whey protein hydrolysates. *Journal of Dairy Science*, *100*(9), 6885–6894. https://doi.org/10.3168/jds.2016-11828

Tanwar, O., Tanwar, L., Shaquiquzzaman, M., Alam, M. M., & Akhter, M. (2014). Structure based virtual screening of MDPI database: Discovery of structurally diverse and novel DPP-IV inhibitors. *Bioorganic & Medicinal Chemistry Letters*, *24*(15), 3447–3451. https://doi.org/10.1016/j.bmcl.2014.05.076

Xie, M.-J., Zhu, M.-R., Lu, C.-M., Jin, Y., Gao, L.-H., Li, L., Zhou, J., Li, F.-F., Zhao, Q. H., Liu, H.-K., Sadler, P. J., & Sanchez-Cano, C. (2017). Synthesis and characterization of oxidovanadium complexes as enzyme inhibitors targeting dipeptidyl peptidase IV. *Journal of Inorganic Biochemistry*, *175*, 29–35. https://doi.org/10.1016/j.jinorgbio.2017.06.014

Zaltariov, M. F., Hammerstad, M., Arabshahi, H. J., Jovanović, K., Richter, K. W., Cazacu, M., Shova, S., Balan, M., Andersen, N. H., Radulović, S., Reynisson, J., Andersson, K. K., & Arion, V. B. (2017). New iminodiacetate-thiosemicarbazone hybrids and their copper(II) complexes are potential ribonucleotide reductase R2 inhibitors with high antiproliferative activity. *Inorganic Chemistry*, *56*(6), 3532–3549. https://doi.org/10.1021/acs.inorgchem.6b03178